Sustainable Energy & Fuels

REVIEW

Check for updates

Cite this: *Sustainable Energy Fuels*, 2019, **3**, 366

Recent progress of transition metal nitrides for efficient electrocatalytic water splitting

Xiang Peng,[a] Chaoran Pi,[b] Xuming Zhang,[b] Shuai Li,[c] Kaifu Huo*[bd] and Paul K. Chu*[e]

Received 28th October 2018
Accepted 7th December 2018

DOI: 10.1039/c8se00525g

rsc.li/sustainable-energy

The hydrogen evolution reaction (HER) and oxygen evolution reaction (OER) constitute the two main processes in electrochemical water splitting to produce high-purity hydrogen and oxygen as alternatives to fossil fuel. Catalysts are crucial to high-efficiency conversion of water to hydrogen and oxygen. Although transition metal nitrides (TMNs) are promising HER and OER catalysts due to the unique electronic structure and high electrical conductivity, single-phase nitrides have inferior activity compared to Pt-group metals because of the unsatisfactory metal–hydrogen (M–H) bonding strength. TMNs-based composites in combination with other metals, carbon materials, and metallic compounds have been demonstrated to possess improved catalytic properties because the modified electronic structure leads to balanced M–H bonding strength, synergistic effects, and improved electrochemical stability. Herein, recent progress pertaining to TMNs is reviewed from the perspective of advanced catalysts for electrochemical water splitting. The challenges and future opportunities confronting TMNs-based catalysts are also discussed.

1. Introduction

Because of the limited fossil fuel resource as well as environmental concern, development of clean and renewable alternatives to fossil fuels is important.[1–3] Among the various strategies, hydrogen has attracted significant attention because of its high gravimetric energy density beyond that of known fuels, compatibility with electrochemical processes, and energy

[a]*School of Materials Science and Engineering, Wuhan Institute of Technology, Wuhan 430205, China*

[b]*The State Key Laboratory of Refractories and Metallurgy and Institute of Advanced Materials and Nanotechnology, Wuhan University of Science and Technology, Wuhan 430081, China*

[c]*Department of Architecture and Civil Engineering, City University of Hong Kong, Tat Chee Avenue, Kowloon, Hong Kong, China*

[d]*Wuhan National Laboratory for Optoelectronics (WNLO), School of Optical and Electronic Information, Huazhong University of Science and Technology, Wuhan 430074, China. E-mail: kfhuo@hust.edu.cn*

[e]*Department of Physics and Department of Materials Science and Engineering, City University of Hong Kong, Tat Chee Avenue, Kowloon, Hong Kong, China. E-mail: paul.chu@cityu.edu.hk*

Xiang Peng received his BS in Metal Materials Engineering from Wuhan University of Science and Technology in 2011 and PhD in Physics and Materials Science from City University of Hong Kong in 2017. He was a postdoctoral fellow at City University of Hong Kong from 2017 to 2018. He is now a distinguished professor of Materials Science and Engineering at Wuhan Institute of Technology. His research interests focus on synthesis of functional nanomaterials and their applications in energy storage and conversion.

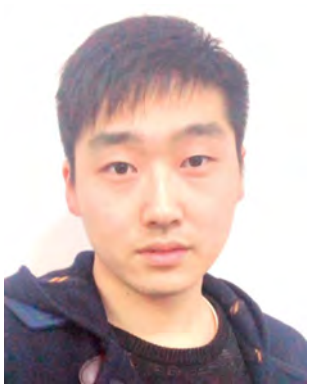

Chaoran Pi is a PhD candidate in the State Key Laboratory of Refractories and Metallurgy at Wuhan University of Science and Technology under the supervision of Prof. Kaifu Huo. His research interest focuses on the design and synthesis of nanostructured transition metal nitrides for electrocatalysis application.

conversion without CO_2 emission.[4] In order to replace existing fossil fuel, effective and economical production of high-purity hydrogen gas is the key. In the industry, hydrogen is generally produced by expensive and energy-demanding steam reformation of hydrocarbons derived from fossil fuels. This process inevitably gives out a large amount of CO_2 and therefore, green techniques which can produce hydrogen on a large scale are attractive for practical applications. Electrocatalytic water splitting is an environmentally friendly and carbon-free alternative if the power can be derived from renewable energy sources such as solar, wind, hydro, or geothermal energy.[5–7] Currently, noble metals such as Pt, Pd, Ir, Ru and their alloys are the common electrocatalysts, but their scarcity and high cost have limited industrial production.[8–12] Hence, there is tremendous interest in developing alternative non-noble-metal based electrocatalysts for efficient water splitting.

Transition metal compounds have attracted increasing interest in the photo and electrochemistry and energy fields, for example, metal-ion batteries,[13–16] supercapacitors,[17–20] solar cells,[21–24] sensors,[25–27] and photo/electro-catalysts[28–36] because of the multi-valence states, special electronic structure, and physical properties. Many kinds of non-noble-metal compounds including metal oxides, carbides, sulfides, phosphides, *etc.* have been proposed as electrocatalysts for HER and OER in water splitting[37–43] and transition metal nitrides (TMNs) have attracted considerable attention due to their unique metal-like physical and chemical characteristics and electronic structure.[44] Introduction of nitrogen atoms to transition metals increases the d-electron density and contraction of the d-band makes the electronic structure of TMNs resembling that of noble metals such as Pd and Pt up to the Fermi level.[45] Besides the metallic conductivity, TMNs have high corrosion resistance boding well for electrocatalytic water splitting in acidic and

Xuming Zhang received his PhD in Materials Science and Engineering from City University of Hong Kong in 2015 and worked for one year as a senior research associate in the Plasma Laboratory at City University of Hong Kong under the supervision of Prof. Paul K. Chu. He is now working as professor in Wuhan University of Science and Technology. His research interests are synthesis of nanomaterials for electrochemical application including electrocatalysis, supercapacitors and biosensing.

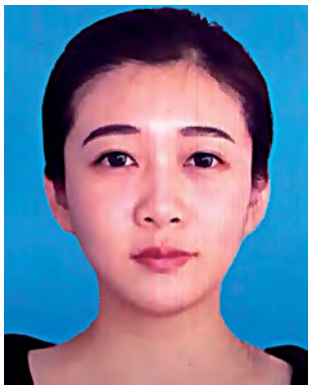

Shuai Li is studying for a Master's degree at City University of Hong Kong and part-time RA at the Department of Architecture and Civil Engineering. Her research focuses on Geography information systems, functional materials and information systems.

Kaifu Huo received his BS in Applied Chemistry from China University of Petroleum in 1997 and PhD in Physical Chemistry from Nanjing University in 2004. He is currently a Professor in the National Laboratory for Optoelectronics at Huazhong University of Science and Technology. He is an associate editor of Nanoscience and Nanotechnology Letters (NNL). He has authored/co-authored more than 100 papers in international refereed journals, which are cited more than 4000 times (current H-index: 36). His main research activities encompass bioactive nanomaterials and nanostructured electrode materials for electrochemical biosensors and energy storage devices.

Paul K. Chu received his PhD in chemistry from Cornell University. He is Chair Professor of Materials Engineering in Department of Physics and Department of Materials Science and Engineering at City University of Hong Kong. He is a Fellow of American Physical Society (APS), Institute of Electrical and Electronics Engineers (IEEE), Hong Kong Institution of Engineers (HKIE), and Hong Kong Academy of Engineering Sciences (HKAES). His research interests are quite diverse encompassing plasma surface engineering, materials science and engineering, surface science, and functional materials. He is a highly cited researcher in materials science according to Clarivate Analytics (Web of Science).

alkaline solutions. K. Sasaki *et al.* have studied the electrocatalytic activity of molybdenum nitride (MoN) in HER.[46] However, the catalytic performance for this single-phase nitride is unsatisfactory because the onset potential is −157 mV (*vs.* RHE). They have further modified MoN by introducing Ni atoms to form Ni–Mo binary nitride. In the binary nitride system, the Mo–H bonding strength is moderated by neighboring Ni atoms resulting in improved catalytic activity (onset potential of −78 mV *vs.* RHE) and structural stability in acidic media compared to the single-phase nitride.[47] In addition, there are synergistic effects between TMNs and non-metal atoms because of modification of the electron density distribution in the hybrid materials with large dispersity and more exposed active sites consequently giving rise to good electrocatalytic activity and stability. For example, Shao *et al.* have prepared tungsten nitride coupled with nitrogen-rich porous graphene-like carbon with high catalytic activity which needs only 132 mV to drive the current density of 10 mA cm^{-2} and good stability.[48]

In this mini-review, the structure and physical properties of TMNs are described and recent development of TMNs-based electrocatalysts is discussed from the viewpoint of water splitting. Several types of TMNs-based electrocatalysts including single-phase TMNs, binary TMNs, TMNs/carbon composites, TMNs/metal and TMNs/metal compounds composites are described. In addition, the challenge and prospect of TMNs-based electrocatalysts are presented from the perspective of high-performance water splitting.

2. Structure and physical properties of TMNs

2.1 Structure of TMNs

Group IVB-VIB TMNs possess unique physical and chemical properties, which are often considered "interstitial alloys" by integrating nitrogen atoms into the interstitial sites of the parent metals.[49–53] As a result, the metal atoms are close-packed or near close-packed thus giving TMNs the attractive electrical conductivity.[54,55] Fig. 1 shows the common crystal structures of TMNs, including face-centered cubic (fcc), hexagon-closed packed (hcp), and simple hexagonal (hex) structures formed by the small nitrogen atoms occupying interstitial positions. Table 1 shows the typical crystal structures of TMNs with different number of nitrogen atoms and transition metals.

2.2 Physical properties of TMNs

There are three different metal-nitrogen (M–N) bonding configurations in TMNs, namely covalent bond, ionic bond, and metallic bond.[68] Covalent bonding produces high hardness, brittleness and better tolerance to stress, whereas ionic bonding between the nitrogen atoms and metals in TMNs results in a contraction of the metals d-band making the electronic structure of transition metal similar to that of noble metals such as Pd and Pt, thus providing excellent electrocatalytic performance.[45] Metallic bonding in TMNs provides good electron transfer and high resistance against corrosion. Generally, TMNs have small electrical resistivity, for instance, TiN (27 μΩ cm), VN (65 μΩ cm), NbN (60 μΩ cm), and ZrN (24 μΩ cm).[85] In fact, the electrical resistivity of the TMNs is influenced by the non-metal/metal ratio that the electrical resistivity decreases

Table 1 Crystal structures of common transition metal nitrides

Transition metals	Nitrides	Crystal structures	Ref.
Ti	TiN	Cubic	56–60
Nb	NbN	Hexagonal	61
	Nb_4N_5	Tetragonal	62 and 63
V	VN	Cubic	64–68
W	WN	Hexagonal	69
	W_2N	Cubic	70 and 71
Mo	MoN	Hexagonal	72 and 73
	Mo_2N	Cubic	70 and 74
Ta	Ta_3N_5	Orthorhombic	75 and 76
	TaN	Cubic	71 and 77
	Ta_2N	Hexagonal	77
Zr	ZrN	Cubic	72, 76 and 78
Ga	GaN	Hexagonal	73 and 79
Cr	CrN	Cubic	71 and 80
Fe	FeN	Cubic	81 and 82
	Fe_3N	Hexagonal	81 and 83
Co	Co_2N	Orthorhombic	79
	Co_3N	Hexagonal	79
	Co_4N	Cubic	79
Ni	Ni_3N	Hexagonal	79 and 83
	Ni_2N	Tetrahedral	83 and 84

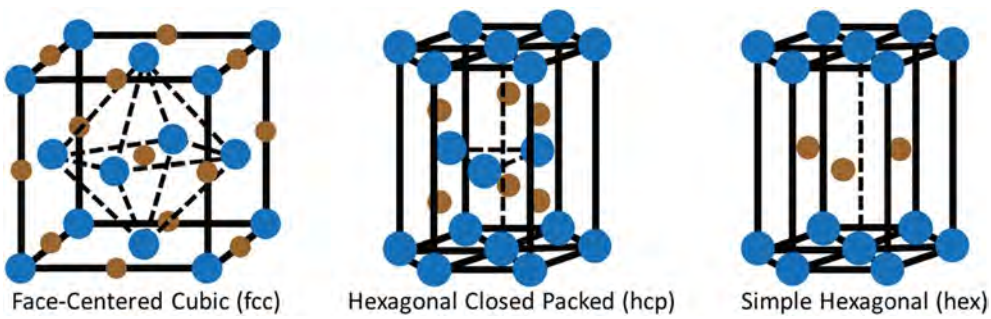

Fig. 1 Common crystal structures of TMNs. The blue balls represent transition metal atoms and brown balls represent nitrogen atoms (reproduced with permission[44] and copyrighted 2016, Wiley-VCH).

with increasing the non-metal content at room temperature.[85] Especially, superconductivity is common among all fcc TMNs of IVB and VB groups.[85] Moreover, TMNs have high chemical stability and are not readily corroded in diluted acidic or alkaline solutions. These properties make them more reliable in electrochemical reactions in comparison with the corresponding metals or metal alloys.

3. Preparation of TMNs

The preparation methods of TMNs can be divided into physical methods such as laser ablation, arc discharge, evaporation, and pulsed-laser deposition[86–91] as well as chemical methods. Chemical synthesis is more preferred for TMNs and the methods can be divided into five categories: (1) direct nitridation of the transition metals,[92] (2) nitridation of transition metal oxides,[53,64,66] (3) ammonolysis of metal chlorides,[93,94] (4) solvothermal method,[95,96] and (5) thermal decomposition of polymeric precursors.[97,98]

TMNs are generally prepared by a topochemical process using metal oxides as precursors and N_2, NH_3, urea, and nitrogen-containing organic chemicals as the nitrogen sources. Typically, annealing under N_2 to produce TMNs requires high temperature (>1200 °C).[99] Using supramolecular complexes as nitrogen source to produce TMNs needs several kinds of nitrogen-containing organic chemicals and moreover, the TMNs were formed *via* a slow solid-state process.[100] Compared to these preparation protocols, producing TMNs by thermal ammonia reduction (gas–solid reaction) at a moderate temperature (normally 300–800 °C) by a simple operation is preferred, as schematically shown in Fig. 2. During the conversion process, the nitrides maintain the morphology of the oxides but produce a large number of mesopores on the surface due to volume shrinkage from oxides to the corresponding nitrides. Conversion of transition metal oxides (TMOs) to TMNs by ammonia annealing has been employed to produce TMNs with different morphologies from zero dimension to three dimensions. For example, Peng *et al.* have prepared mesoporous TiN nanotube arrays from TiO_2 nanotube arrays[57,58] and mesoporous VN nanosheets from V_2O_5 nanosheets[64] by ammonia annealing. Gao *et al.* have prepared VN nanowires by nitriding V_2O_5 nanowires[67] and Ma *et al.* have synthesized Mo_2N nanobelts by nitriding the MoO_3 nanobelts precursor.[74] Ta-based TMNs have also been prepared by ammonia reduction after anodization.[101–103] TMOs such as Nb_2O_5, NiO, CoO, Cr_2O_3, Fe_2O_3, and WO_3 have been converted into the corresponding TMNs by thermal nitridation.[104–113] The ammonia annealing method can be applied to single-phase TMNs as well as binary TMNs. Jia *et al.* have prepared Ni_3FeN nanoparticles through thermal treatment of NiFe-layer double hydroxide nanosheets under ammonia at 500 °C and formed an efficient overall water splitting electrocatalyst.[114] Jia *et al.* have reported an efficient bifunctional electrode consisting of $Ni_{0.2}Mo_{0.8}N$ nanorods on Ni foam prepared by topotactic transformation of $NiMoO_4$ nanorods at 550 °C under flowing NH_3.[115]

Recently, ammonia nitriding has been adopted to prepare nitride-based composites by *in situ* phase separation from the complex oxide. Hybrid composites can be produced due to the different bonding energy between the metal atoms and non-metal atoms. For instance, Peng *et al.* have prepared the composite of VN and metallic Co *via* nitriding of the $Co_2V_2O_7$ precursor at a controlled temperature.[65] Li *et al.* have produced a series of mixtures composed of NiCo-based oxides and Ni_3N by ammonia annealing of $NiCo_2O_4$ (ref. 116) and Xiao *et al.* have reported a scalable method to produce two-dimensional (2D) nitrides such as MoN, W_2N, and V_2N by nitriding the corresponding 2D hexagonal oxides under ammonia.[117] As shown in Fig. 3, 2D hexagonal TMOs-coated NaCl (2D h-TMOs@NaCl) is obtained by annealing the metal-based precursors@NaCl powders under Ar at 280 °C.[118] The 2D h-TMOs@NaCl powders are slowly heated in ammonia at 650 °C and during this process, the salt acts as the stabilizer to avoid morphological changes during transformation from TMOs to TMNs.[119] The 2D TMNs@NaCl powders are washed in deionized water and filtered to remove the salts. This method has been demonstrated to produce large and high-quality 2D metal nitride flakes.

The thermal chemical methods utilizing ammonia gas have drawbacks such as the high temperature, long annealing time, as well as toxic precursors. However, physical methods such as magnetron sputtering are suitable for thin film growth but difficult to be applied in fabrication of 3D nanostructures. Fortunately, nanostructured TMOs have been converted into their corresponding TMNs *via* plasma immersion ion implantation (PIII) method which is a 3D surface modification technique at room temperature.[120–122] In addition, the high efficient PIII technique can convert TMOs into TMNs completely in a short time using a radio frequency (RF) nitrogen plasma.[123] For example, Zhang *et al.* have prepared CoN and NiMo-based nitrides by RF PIII.[123,124] Other TMNs such as TiN,[125–127] Ni_3N,[128] TaN,[129–131] GaN,[132] and AlN[133,134] have also been prepared *via* plasma treatment.

Fig. 2 Schematic diagram illustrating the fabrication of TiN nanotube arrays from TiO_2 nanotube arrays by ammonia nitridation (reproduced with permission[58] and copyrighted 2013, The Royal Society of Chemistry).

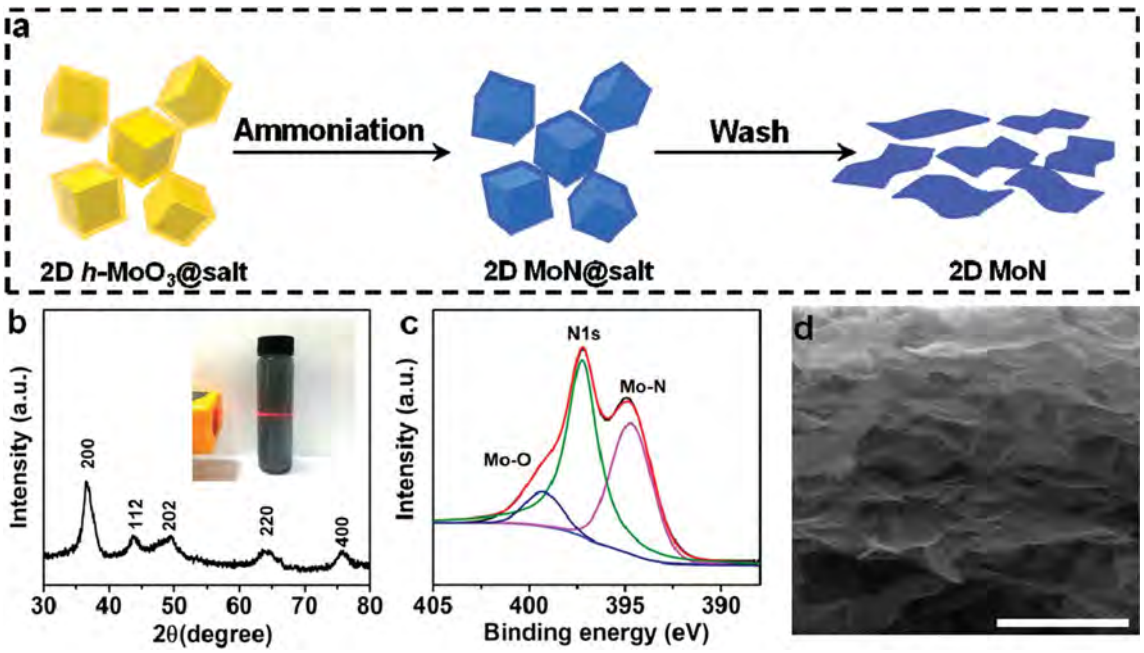

Fig. 3 (a) Schematic illustration of synthesis of 2D MoN. (b) XRD pattern of 2D MoN powders. The inset shows the Tyndall effect of the 2D MoN colloidal solution in water demonstrating good dispersity of 2D MoN in water. (c) N 1s and Mo 3p XPS spectra of 2D MoN. (d) SEM image shows the 2D morphology of the synthesized MoN (scale bar, 500 nm). Reproduced with permission[117] and copyrighted 2017, American Chemical Society.

4. Mechanism of electrochemical water splitting

Fig. 4 shows the typical electrochemical water splitting system comprising three components: cathode, anode, and electrolyte. Both the cathode and anode are coated with electrocatalysts to accelerate the water splitting reactions. When an external voltage is applied to the electrodes, water molecules are decomposed into gaseous hydrogen and oxygen on the cathode and anode, respectively. The electrochemical water splitting reaction can be divided into two half-reactions: oxygen evolution reaction (OER) and hydrogen evolution reaction (HER). Considering the different electrolytes in which water splitting takes place, the water splitting reactions can be expressed as follows:

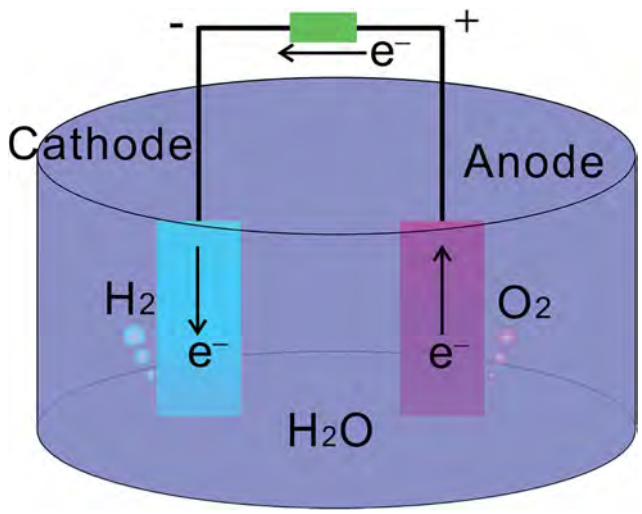

Fig. 4 Schematic diagram of an electrochemical water splitting system.

Total reaction:

$$2H_2O \rightarrow 2H_2 + O_2 \quad (1)$$

In an acidic electrolyte:

$$\text{Cathode: } 4H^+ + 4e^- \rightarrow 2H_2 \quad (2)$$

$$\text{Anode: } 2H_2O \rightarrow 4H^+ + O_2 + 4e^- \quad (3)$$

In an alkaline electrolyte:

$$\text{Cathode: } 2H_2O + 4e^- \rightarrow 2H_2 + 4OH^- \quad (4)$$

$$\text{Anode: } 4OH^- \rightarrow 2H_2O + O_2 + 4e^- \quad (5)$$

HER in acidic media is normally associated with three possible reactions, but in alkaline media, the reaction mechanism is still not well understood.[135] In the acidic media, the first step in HER is the Volmer step: $H^+ + e^- \rightarrow H_{ads}$. During this reaction, a proton absorbs and reacts with an electron to produce an adsorbed hydrogen atom (H_{ads}) on the catalyst surface. In the second step, hydrogen is produced by the Tafel step ($2H_{ads} \rightarrow H_2$) or Heyrovsky step ($H_{ads} + H^+ + e^- \rightarrow H_2$) and then desorbs from the catalyst surface. However, adsorption and removal of H atoms on the electrode surface are competitive processes. Binding energies between the catalyst surface

and H atoms that are neither too large nor too small for the overall HER reaction because weak bonding leads to poor adsorption of the reactant and strong bonding makes it difficult to remove the product. The HER kinetics combines absorption and release of hydrogen atoms assessed by the free energy of hydrogen adsorption (ΔG_H). Theoretically, ΔG_H of Pt is nearly zero and so it is the best hydrogen evolution catalyst in acidic media as verified experimentally. However, Pt is an expensive noble metal with a limited supply thus hindering commercial production and the major challenge is to design and develop non-noble-metal based alternatives with a nearly zero ΔG_H.

OER is the other half reaction in electrochemical water splitting. During OER, oxygen molecules are produced by several proton/electron-coupled procedures.[15–17] To produce an O_2 molecule, a process with four electron transfer is required. However, the OER process occurs *via* multi-step reactions with single-electron transfer in each step. Thus, the energy barriers accumulate at each individual step rendering the OER kinetics sluggish resulting in a large overpotential. In order to overcome the large energy barrier during OER, electrocatalysts with a low overpotential, high stability, and low cost are desirable. Although noble-metal-based materials (such as RuO_2 and IrO_2 (ref. 136 and 137)) have high stability in a wide range of pH in OER, the high cost is the major commercial obstacle. In this respect, carbon-based materials and transition metal-based catalysts including Mn, Co, Ni, and Fe, and their composites are promising alternatives.[138–142]

Table 2 Comparison and summary of recently reported TMNs-based catalysts in electrochemical water splitting

Catalyst	Synthesis approach	Electrolyte	η_1[a] [mV]	η_{10}[b] [mV]	Tafel slope [mV dec^{-1}]	Ref.
HER						
TiN nanowires	N_2 annealing	1 M $HClO_4$	92		54	99
Bulk TiN	N_2 annealing	1 M $HClO_4$	405		161	99
γ-Mo_2N	Urea glass route	0.5 M H_2SO_4		381	100	153
		1 M KOH		353	108	153
		1 M $HClO_4$		∼300		154
MoN/C	NH_3 annealing	0.1 M $HClO_4$	∼280		54.5	46
δ-MoN	NH_3 annealing	0.1 M $HClO_4$		∼420		144
NiN_x	Anion exchanging	1 M KOH	100		127	155
Ni_3N/Ni-foam	Supramolecular complexes reduction	1 M KOH		∼150	120	100
CoN_x	Anion exchanging	1 M KOH	200		151	155
$CoNiN_x$	Anion exchanging	1 M KOH	150		130	155
WN/rGO	NH_3 annealing	0.5 M H_2SO_4		265	118	156
P-WN/rGO	NH_3 annealing	0.5 M H_2SO_4		85	54	156
Ni_3N nanoparticles	NH_3 annealing	1 M KOH			67	114
Ni_3FeN	NH_3 annealing	1 M KOH		45	75	157
Ni_3FeN nanoparticles	NH_3 annealing	1 M KOH		158	42	114
Bulk Ni_3FeN	NH_3 annealing	1 M KOH			48	114
Co_3FeN_x	NH_3 annealing	1 M KOH		23	94	158
$FeNi_3N$/Ni foam	NH_3 annealing	1 M KOH		75	98	159
$NiMoN_x$/C	NH_3 annealing	0.1 M $HClO_4$	∼170		35.9	46
$Co_{0.6}Mo_{1.4}N_2$	NH_3 annealing	0.1 M $HClO_4$		190		144
OER						
Ni_3N nanosheets	NH_3 annealing	1 M KOH			45	152
Bulk Ni_3N	NH_3 annealing	1 M KOH			85	152
Ni_3N nanoparticles	NH_3 annealing	1 M KOH		430	64	114
Ni_3N/Ni-foam	Supramolecular complexes reduction	1 M KOH		∼370	65	100
CoN nanowires	Plasma treatment	1 M KOH		290	70	123
Co_2N	NH_3 annealing	1 M KOH		390	72	69
Co_3N	NH_3 annealing	1 M KOH		370	80	69
Co_4N nanowires	NH_3 annealing	1 M KOH		257	44	160
Co_4N	NH_3 annealing	1 M KOH		330	58	69
Ni_3N NA/CC	NH_3 annealing	1 M $KHCO_3$		540@20mA cm^{-2}	162	161
Ni_3N@Ni-Ci NA/CC	NH_3 annealing	1 M $KHCO_3$		400@20mA cm^{-2}	143	161
Co_3FeN_x	NH_3 annealing	1 M KOH		222@20mA cm^{-2}	46	158
$FeNi_3N$/Ni foam	NH_3 annealing	1 M KOH		202	40	159
Ni_3FeN	NH_3 annealing	1 M KOH		223	40	157
Ni_3FeN nanoparticles	NH_3 annealing	1 M KOH		280	46	114
Bulk Ni_3FeN	NH_3 annealing	1 M KOH		320	67	114

[a] Overpotential required for generating a hydrogen (oxygen) evolution current density of 1 mA cm^{-2}. [b] Overpotential required for generating a hydrogen (oxygen) evolution current density of 10 mA cm^{-2}.

TMNs are found to be excellent electrocatalysts for water splitting. Introducing of nitrogen to transition metals modifies the electronic structure of the metals by increasing the density of state (DOS) near the Fermi level and the redistributions of DOS in turn produce electrocatalytic properties similar to those of noble metals.[44] Consequently, metal nitrides have higher electrocatalytic activities in electrochemical catalytic reactions than the corresponding pure metals.[143,144]

However, similar to transition-metal-based carbides, phosphides, and sulfides, metal nitrides also tend to be converted into the corresponding metal oxides slightly on the surface during the OER due to electrochemical oxidation.[65,145]

5. TMNs based catalysts for electrochemical water splitting

Many TMNs such as single-phase nitrides, binary nitrides, and nitrides-based composites have been investigated as catalysts in both HER and OER and they show good activity and stability in a wide pH range.

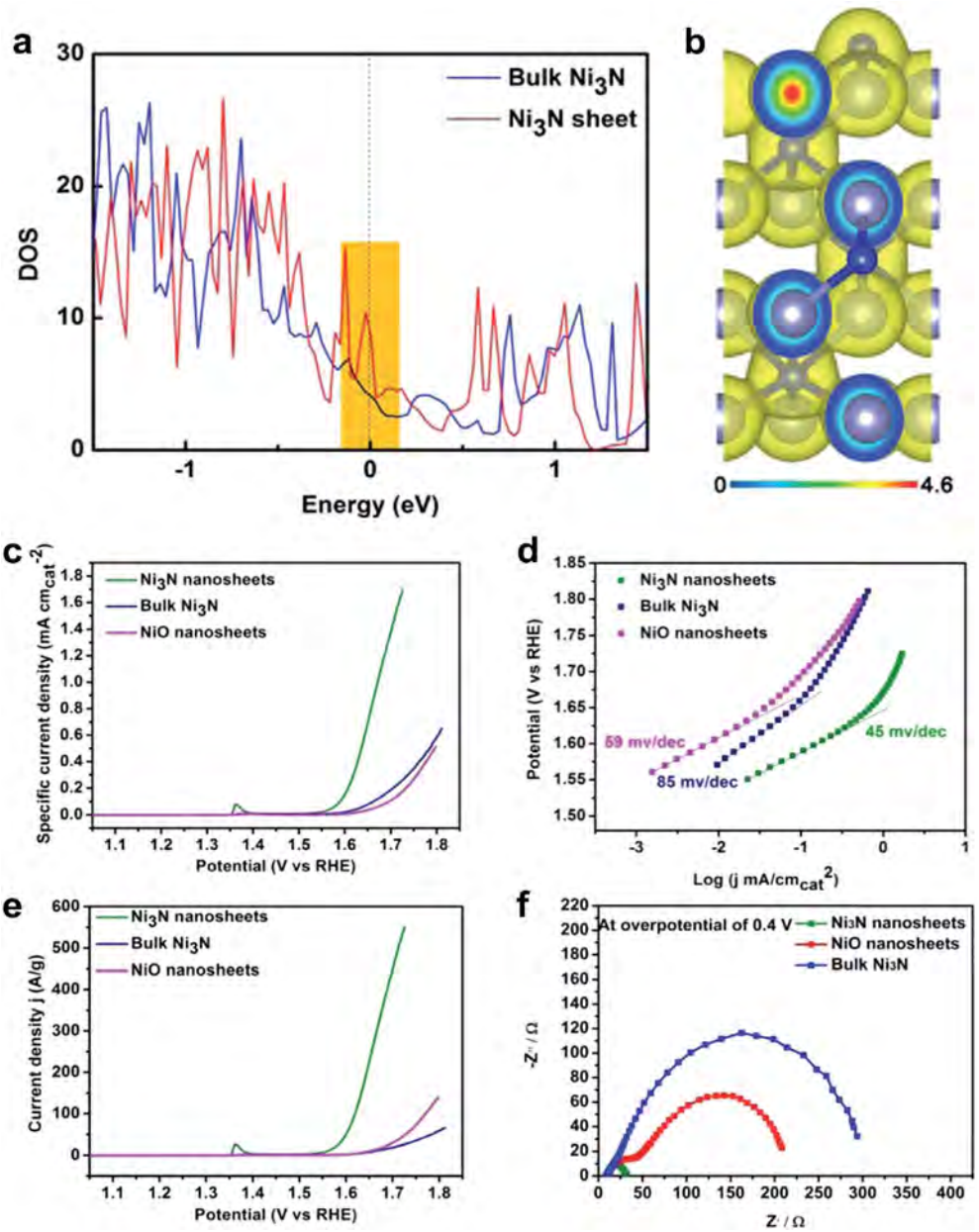

Fig. 5 (a) Calculated density of states of the bulk Ni_3N and Ni_3N sheet. The Fermi level is set at 0 eV. (b) Charge density waves of the Ni_3N sheet plotted from 0 (blue) to 4.6 e $Å^{-3}$ (red). (c) Normalized polarization curves of the Ni_3N nanosheets, bulk Ni_3N, and NiO nanosheets according to the BET surface area of the electrocatalysts. (d) Corresponding Tafel plots of the Ni_3N nanosheets, bulk Ni_3N, and NiO nanosheets. (e) Mass activity of the Ni_3N nanosheets, bulk Ni_3N, and NiO nanosheets at different applied potentials. (f) Nyquist plots of the Ni_3N nanosheets, bulk Ni_3N and NiO nanosheets. Reproduced with permission[152] and copyrighted 2015, American Chemical Society.

5.1 Single-phase TMNs

Single-phase TMNs such as MoN, VN, WN, NbN, TiN, Ni_3N *etc.* have been studied in electrochemical water splitting and show promising catalytic ability. The comparison and summary of recently reported TMNs-based catalysts are presented in Table 2. Xie *et al.* have shown metallic MoN nanosheets with atomic thickness to be an efficient platinum free electrocatalyst in HER[146] and Mo atoms on the surface act as active sites to reduce protons to hydrogen. This work provides fundamental understanding and is helpful to optimize the surface structure to achieve high HER activity. Murthy *et al.* have fabricated several metal-doped Mo_3N_2 films using magnetron co-sputtering and evaluated the HER activity in a phosphate buffered medium (pH = 5).[147] Both the onset potential and stability of the Mo_3N_2 films are enhanced in a near-neutral medium.

Tungsten-based compounds exhibit a similar behavior as molybdenum-based compounds. Moreover, tungsten nitrides have better corrosion resistance and stability under neutral and higher pH conditions compared to tungsten carbides.[148,149] Shi *et al.* have fabricated WN nanorod arrays (NA) by nitridation of the corresponding WO_3 NA precursors.[150] The WN NA serving as a robust integrated 3D hydrogen evolution cathode can be operated from pH of 0 to 14 with good catalytic performance and durability. Ren *et al.* have prepared porous WN nanowires arrays (NWs) by N_2 plasma treatment of WO_x NWs for a short time (10 min). The WN NWs show enhanced HER electrocatalytic activity and stability in both acidic and alkaline media. Their strategy suggests a facile way to fabricate active and stable catalysts for HER.[151]

TMNs have potential application in OER. Xu *et al.* have reported metallic Ni_3N nanosheets as an efficient OER electrocatalyst.[152] The first-principles calculation and electrical transport measurements suggest that Ni_3N has an improved electron density by dimensional confinement resulting in intrinsically metal-like characteristics (Fig. 5a and b). As a result, the Ni_3N nanosheets show a small Tafel slope of 45 mV dec^{-1} which is better than those of bulk Ni_3N (85 mV dec^{-1}) and NiO nanosheets (59 mV dec^{-1}) as indicated in Fig. 5. The excellent OER performance can be attributed to the change in the surface electron density enhancing the electrical conductivity based on the metallic behavior.

5.2 Binary metal nitrides

Although single-phase TMNs have promising electrical conductivity and activity in electrochemical water splitting, single-phase TMNs have steady M–H bonding strength which is either higher or lower than that of Pt-based catalysts resulting in inferior activity compared to Pt-group metals.[162] Moreover, the long term stability of some single-phase nitrides are not satisfactory under extreme electrochemical conditions.[163] A simple way to improve the electrochemical activity of single-phase TMNs is to alter the electronic properties by introducing another metal to weaken M–H or strengthen M–H bonding.[164]

The "volcano plot" elucidates the HER theory of single transition metals.[148,165] Navarro-Flores *et al.* have proposed a synergetic mechanism to account for the enhanced kinetics in hydrogen evolution observed from NiMo, NiW, and NiFe bimetallic carbide alloys.[166] The binary metal nitrides show a similar electrocatalytic behavior. Chen *et al.* have synthesized NiMo nitride nanosheets on a carbon substrate ($NiMoN_x$/C) and demonstrated high HER electrocatalytic activity with a low overpotential and small Tafel slope.[46] The nanostructured cobalt molybdenum nitride ($Co_{0.6}Mo_{1.4}N_2$) reported by P. G. Khalifah *et al.* shows high activity and stability in HER under acidic conditions that a small overpotential of 200 mV is

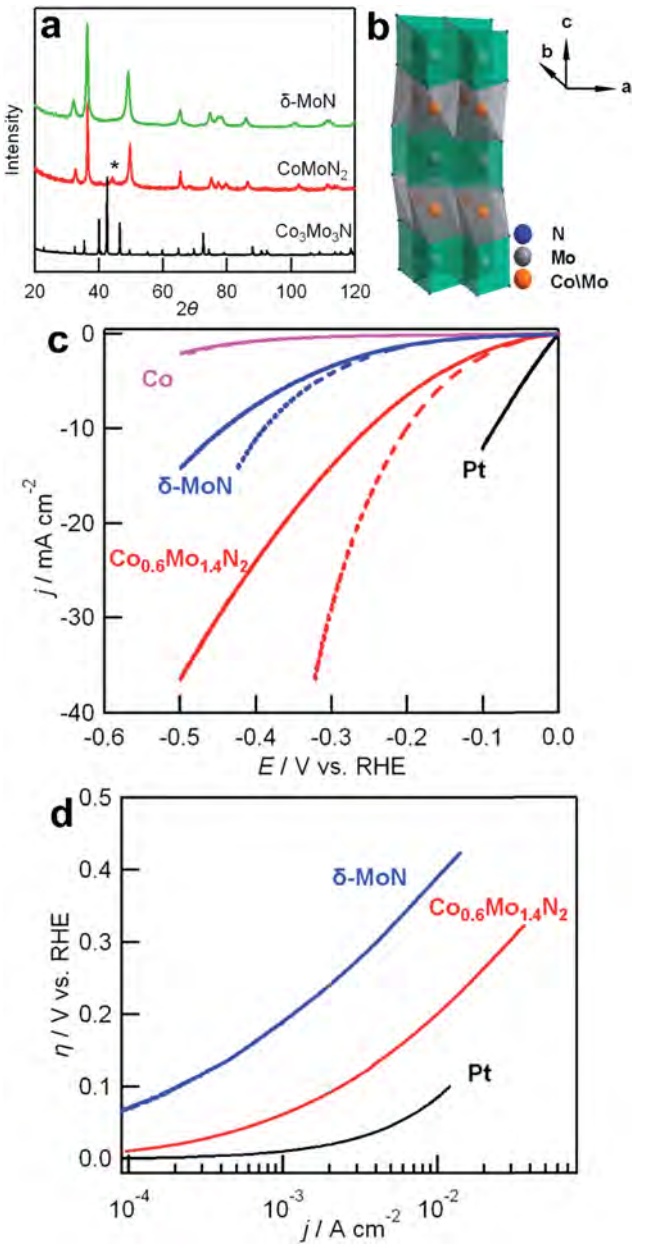

Fig. 6 (a) X-ray powder diffraction patterns of Co_3Mo_3N, $CoMoN_2$, and δ-MoN. The asterisk marks the impurity peak of cobalt metal. (b) Four-layered crystal structure of $CoMoN_2$. (c) Polarization curves of Co, δ-MoN, $Co_{0.6}Mo_{1.4}N_2$ and Pt in H_2-saturated 0.1 M $HClO_4$ with (dashed line) and without (solid line) *iR* correction. (d) Corresponding Tafel plots at low overpotentials after *iR* correction. Reproduced with permission[144] and copyrighted 2013, American Chemical Society.

accomplished at a current density of 10 mA cm^{-2} for a small catalyst loading of 0.24 mg cm^{-2}, as shown in Fig. 6.[144] Wei *et al.* have prepared bimetallic vanadium–molybdenum nitride (MoVN) thin films for HER and the materials show superior electrocatalytic activity in an alkaline electrolyte in contrast to bare VN and Mo_2N in addition to excellent long-term durability. This study reveals the potential of bimetallic TMNs as high-performance HER catalysts.[167]

Catalysts based on binary TMNs perform well in overall water splitting. Wang *et al.* have fabricated a three-dimensional porous $NiCo_2N$ on nickel foam and both OER and HER are enhanced as exemplified by small overpotentials of 0.29 and 0.18 V at 10 mA cm^{-2}, respectively.[168] Yan *et al.* have designed and prepared porous interconnected iron-nickel nitride nanosheets on a carbon fiber cloth with a low mass loading of 0.25 mg cm^{-2} and the materials exhibit excellent catalytic activity in OER with an overpotential of 232 mV at 20 mA cm^{-2} and HER with an overpotential of 106 mV at 10 mA cm^{-2}.[169] The results suggest a new route to prepare low-cost and efficient bifunctional catalysts for overall water splitting. Wang *et al.* have synthesized Ni_3Fe layered double hydroxides (LDHs) precursors on the nickel foam (Ni_3Fe LDHs/NF) by a typical hydrothermal reaction followed by high temperature annealing under NH_3 to obtain Ni_3FeN on Ni foam (Ni_3FeN/NF).[157] The nanosheet structure is preserved after the thermal treatment and excellent conductivity is observed. The Ni_3FeN/NF delivers good performance in both OER and HER and can be directly used in electrochemical water splitting.

5.3 TMNs/carbon composites

Carbon based materials, such as graphene, carbon nanotubes, and carbon nanosheets, are excellent conductive supports for electrocatalysts. Firstly, the carbon materials not only prevent the catalysts from aggregating but also increase the dispersion of active sites.[170–172] Secondly, coupling TMNs with carbon materials is found to create a synergistic effect between the components which can modulate the electron density as well as the distribution of the electronical potentials of the composite to balance the hydrogen surface adsorption/desorption behavior, thus enhancing the electrocatalytic properties.[173] Thirdly, the carbon species around the TMNs serve as a mask to protect against corrosion. Therefore, TMNs combined with carbon materials have demonstrated superior electrocatalytic activity in acidic and alkaline media.[46,154,173,174] Chen *et al.* have prepared the $NiMoN_x$/C catalyst by reduction of ammonium molybdate [$(NH_4)_6Mo_7O_{24}\cdot 4H_2O$] and nickel nitrate ($Ni(NO_3)_2\cdot 4H_2O$) and it exhibits excellent activity in HER with a small overpotential, large exchange current density, and small Tafel slope (Fig. 7).[46] The $NiMoN_x$/C nanosheets show high corrosion resistance in acidic media due to the protection by carbon. Ojha *et al.* have fabricated FeN_x and Mo_2N nanocomposites *in situ* on N-doped CNTs and investigated the synergistic effects of Mo_2N

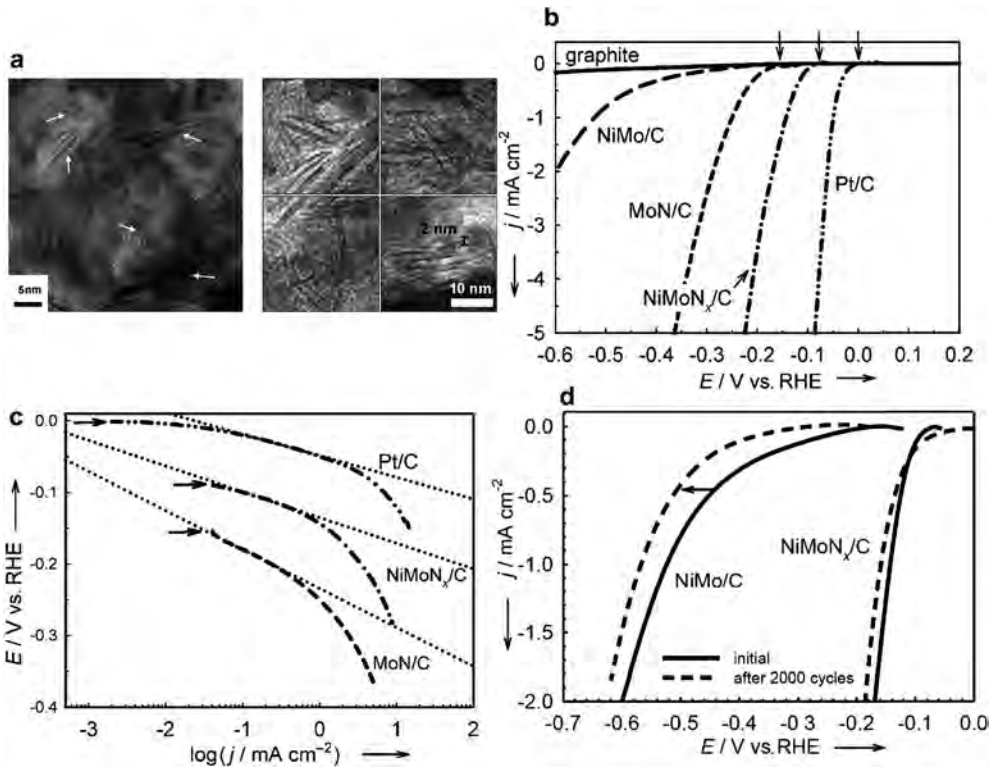

Fig. 7 (a) TEM images of exfoliated $NiMoN_x$ nanosheets prepared by treating the NiMo/C in NH_3 at 700 °C. (b) Polarization curves and (c) corresponding Tafel plots of MoN, $NiMoN_x$, Pt/C catalysts, and graphite (XC-72) in 0.1 M $HClO_4$ (scanning rate of 2 mV s^{-1}). (d) Polarization curves of $NiMoN_x$/C and H_2-reduced NiMo/C before and after potential sweeps for 2000 cycles. Reproduced with permission[46] and copyrighted 2012, Wiley-VCH.

and FeN_x for HER.[175] FeN_x and Mo_2N anchored on the conductive N-doped CNTs reduce the internal contact resistance thus facilitating charge transfer leading to high electrocatalytic HER activity.

Carbon-supported TMNs composites are appropriate for overall water splitting. Chen *et al.* have used a self-template route to fabricate a unique hybrid composite by encapsulating cobalt nitride ($Co_{5.47}N$) nanoparticles in three-dimensional (3D) N-doped porous carbon ($Co_{5.47}N$ NP@N-PC) polyhedral to produce active bifunctional electrocatalyst.[176] $Co_{5.47}N$ NP@N-PC as both the cathode and anode in alkaline solutions can drive the overall water splitting reaction with a current density of 10 mA cm^{-2} at a cell voltage of only 1.62 V, which is superior to that of the Pt/IrO_2 couple. The excellent electrocatalytic activity of $Co_{5.47}N$ NP@N-PC can be ascribed to the high conductivity of the $Co_{5.47}N$, electronic modulation of N-doped carbon towards $Co_{5.47}N$, and the hierarchically porous structure.

5.4 TMNs/metal and TMNs/metal compounds composites

Guided by the "volcano plot", heterostructures composed of TMNs and metals or metal compounds are desirable to balance the M–H bonding strength to enhance electrochemical catalysis due to the interaction at the interface of TMNs and metals. Morozan *et al.* have reported the synergetic effects between Mo_2N nanoparticles and gold.[177] This approach combines Mo having a higher M–H bonding strength with gold having a lower M–H bonding strength, each component being selected to catalyze a targeted step of the HER, thus leading to improved HER activity in acidic medium. Synergetic effects have also been

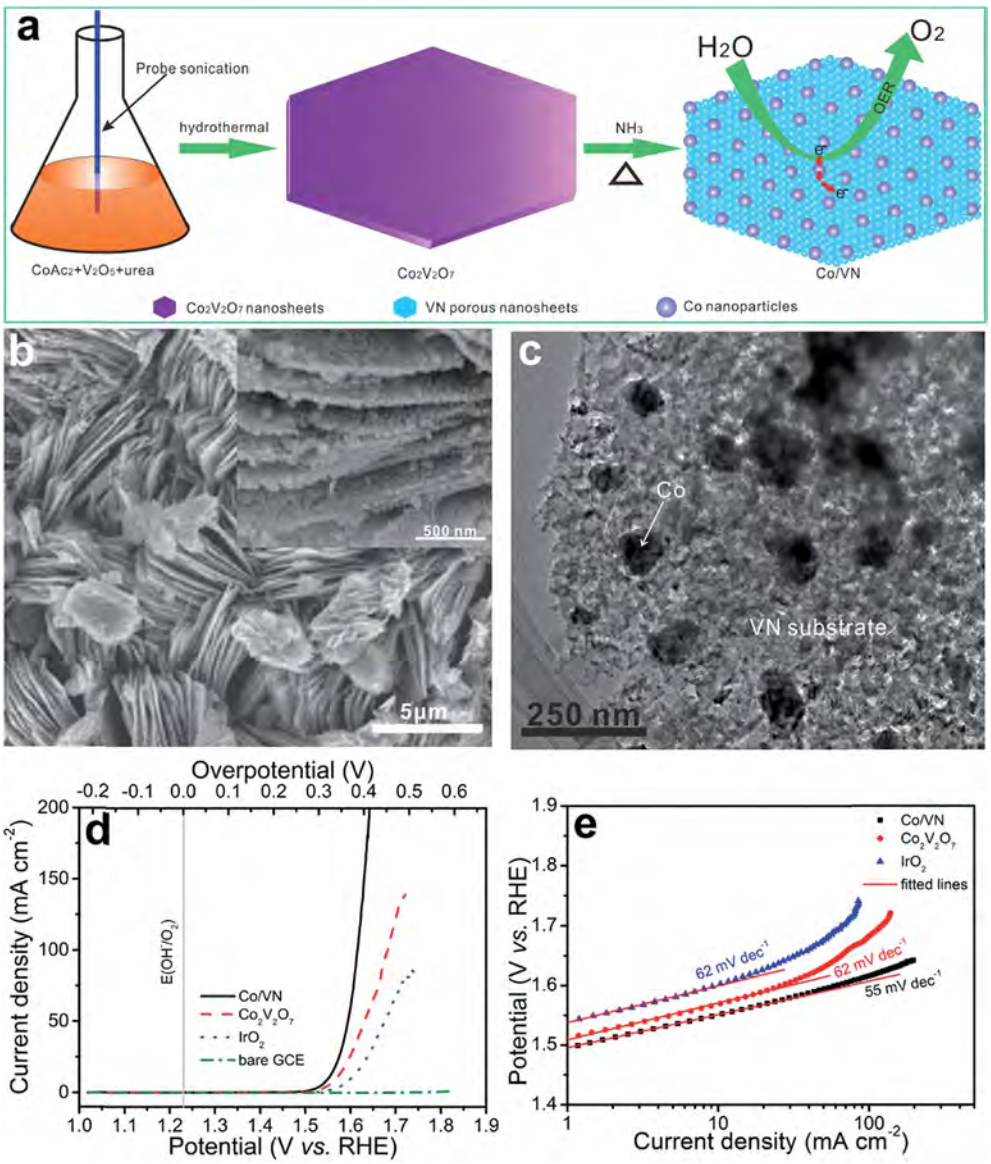

Fig. 8 (a) Schematic illustration of the preparation of porous Co/VN nanosheets in high-performance OER. (b) SEM images and (c) TEM image of Co/VN. (d) Polarization curves of Co/VN, $Co_2V_2O_7$, and commercial IrO_2 electrocatalysts compared to the bare glassy carbon electrode. (e) Corresponding Tafel plots of Co/VN, $Co_2V_2O_7$, and commercial IrO_2 electrocatalysts. Reproduced with permission[65] and copyrighted 2017, Elsevier.

observed from non-noble-metals and TMNs. Peng *et al.* have prepared metallic Co nanoparticles embedded in the VN composite (Co/VN) as shown in Fig. 8.[65] Phase separation occurs during nitriding due to the different bonding energy between the metal atoms and non-metal atoms. The Co/VN composite has good OER activity as demonstrated by a small overpotential of 320 mV at a current density of 10 mA cm^{-2} as well as a small Tafel slope of 55 mV dec^{-1}. Excellent stability after 2000 cyclic voltammetry cycles at a large current density of 200 mA cm^{-2} with an overpotential shift of only 34 mV is demonstrated. The non-noble-metal/TMNs composite with good OER performance and low cost indicates promise in high-efficiency OER in alkaline media.

Composites based on TMNs and other transition metal compounds such as transition metal carbides, nitrides, sulfides, and oxides have been investigated as water splitting electrocatalysts due to the modified M–H bonding strength and synergetic effects among the components.[116,145,175,178–181] The synergistic effects rendered by TMNs and transition metal carbides have been shown to yield excellent HER activity both experimentally and theoretically. Charge transfer at the interface between TMNs and transition metal carbides facilitates hydrogen evolution and more importantly, the free energy of hydrogen adsorption at the interface between these composite is very close to that of the commercially available Pt/C catalyst, suggesting practical application in electrocatalytic water splitting.[179] Recently, our group has fabricated $NiCoO_2$/CoO/Ni_3N composite nanosheet arrays (NiCoON NSAs/NF) *in situ* on the 3D nickel foam, as shown in Fig. 9a.[116] There are more active sites due to the oxygen vacancies on NiCoON NSAs after the treatment with NH_3 and the face-centered cubic $NiCoO_2$ enhances formation of active Ni–Co layered hydroxide/oxyhydroxide species (NiOOH) in comparison with spinal $Ni_xCo_{3-x}O_4$ during the electrochemical process. Furthermore, the

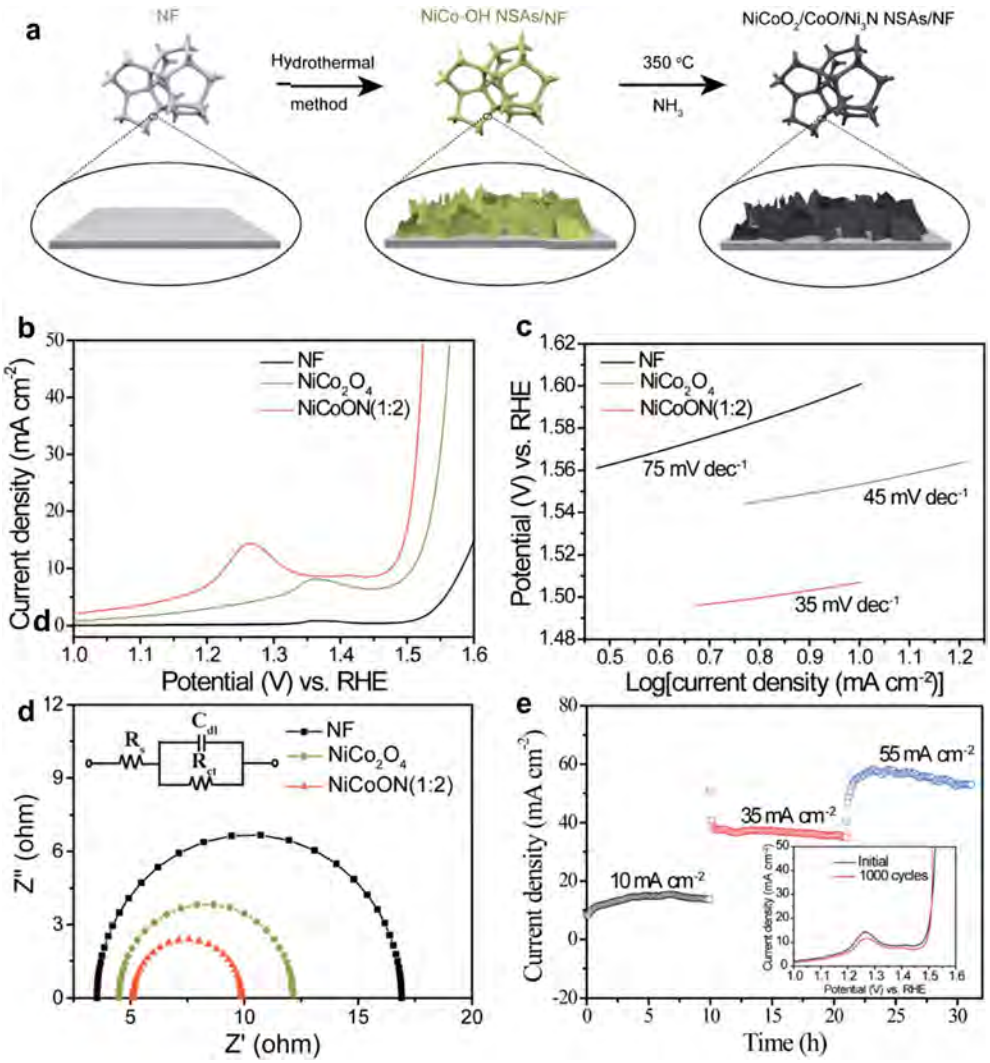

Fig. 9 (a) Schematic illustration of the synthesis of NiCoON ($NiCoO_2$/CoO/Ni_3N) on the NF. (b) OER polarization curves (*iR*-compensated), (c) Tafel plots and (d) Nyquist plots of the NF, $NiCo_2O_4$ NSAs/NF, and NiCoON (1 : 2) NSAs/NF in 1.0 M KOH. (e) Chronopotentiometric response of NiCoON (1 : 2) NSAs/NF at different current densities (10, 35, 55 mA cm^{-2}) in 1.0 M KOH for 30 h. The inset shows the *iR* compensated polarization curves of NiCoON (1 : 2) NSAs/NF before and after 1000 cycles of CV in 1.0 M KOH. Reproduced with permission[116] and copyrighted 2018, Elsevier.

Ni^{3+}-rich surface incorporated with Co facilitates the formation of β-NiOOH. Consequently, in the alkaline solution, the NiCoON nanocomposite has excellent catalytic OER properties (Fig. 9b–e) such as a small overpotential of 247 mV (at 10 mA cm^{-2}) and Tafel slope of 35 mV dec^{-1}, which are better than those of $Ni_xCo_{3-x}O_4$ and most Ni- and Co-based catalysts.

6. Conclusion and outlook

Electrochemical water splitting to produce high-purity hydrogen and oxygen with the aid of electrocatalysts is an environmentally friendly and economic strategy to generate energy and mitigate the use of fossil fuel. In this mini-review, recent progress pertaining to the development and application of TMNs as non-noble-metal and low-cost electrocatalysts in water splitting is described. TMNs such as W_xN, Mo_xN, TiN, Ni_xN, Fe_xN, Co_xN, as well as their binary and composites possess excellent physicochemical properties such as high electrical conductivity and unique electronic structure giving rise to the outstanding performance in electrochemical water splitting. Owing to the modified electronic structure and moderated M–H bonding strength, binary nitrides and TMNs-based composites deliver enhanced performance compared to single-phase nitrides.

Although considerable development has been achieved from TMNs electrocatalysts in water splitting, there is much room to improve the catalytic properties of TMNs in HER and OER. Moreover, several fundamental issues need to be better understood in order to design efficient non-noble-metal based catalysts.

(i) Mechanism

A thorough understanding of the mechanism of HER and OER in electrochemical water splitting is crucial to the design and fabrication of high-performance catalysts. Nitride composites combined with metals, carbon materials, or other transition metal compounds have higher electrocatalytic activity than single-phase TMNs possibly due to the balanced M–H bonding strength and synergetic effects between components, but the underlying mechanism is still not fully understood. For example, the interface between the different components in TMNs-metal carbides should be different from that of TMNs-carbon composites due to the different electronic structure between the metal and carbon. The surface/interface and the reaction sites need to be identified *in situ* to fathom the catalytic mechanism.

(ii) Surface engineering

Both HER and OER occur on the surface of the catalysts and therefore, the atomic arrangement and defects in the near surface play crucial role in the water splitting reaction and dominate the electrocatalytic activity. Defects are traps for electrons and limit the charge transfer efficiency thereby impeding the water splitting kinetics. Fortunately, TMNs have metallic conductivity that facilitates high-efficiency charge transfer. To study the active sites and their evolution during water splitting is of great significance in order to understand the electrocatalytic mechanism and life time. It is important to understand the chemical states on the catalyst surface *in situ* and derive the relationship between the surface chemistry and electrochemical performance.

(iii) Long-term stability

Electrocatalytic water splitting is often conducted in either an alkaline or acidic aqueous medium, which can produce surface polarization of TMNs under extreme pH conditions. It is important to protect TMNs-based electrocatalyst from corrosion in the electrolyte in order to maintain the high activity and stability. Heterostructures loaded or embedded with TMNs on various substrates to mitigate the polarization reaction is believed to be an effective strategy to improve the long-term stability.

Conflicts of interest

There are no conflicts to declare.

Acknowledgements

This work was financially supported by National Natural Science Foundation of China (No. 51572100 and 21875080) as well as City University of Hong Kong Strategic Research Grant (SRG) No. 7005105 and Internal Project No. 9678148.

References

1 C. G. Morales-Guio, L.-A. Stern and X. Hu, *Chem. Soc. Rev.*, 2014, **43**, 6555–6569.
2 J. A. Turner, *Science*, 2004, **305**, 972–974.
3 N. S. Lewis and D. G. Nocera, *Proc. Natl. Acad. Sci. U. S. A.*, 2006, **103**, 15729–15735.
4 M. Curry-Nkansah, D. Driscoll, R. Farmer, R. Garland, J. Gruber and N. Gupta, *Freedom CAR & fuel partnership hydrogen production technical team*, 2009.
5 Z. Liu, D. Zeng, X. Gao, P. Li, Q. Zhang and X. Peng, *Sol. Energy Mater. Sol. Cells*, 2019, **189**, 103–117.
6 Z. Liu, Y. Wu, Q. Zhang and X. Gao, *J. Mater. Chem. A*, 2016, **4**, 17604–17622.
7 Z. Liu, X. Zhang, P. Li and X. Gao, *Sol. Energy*, 2018, **174**, 171–188.
8 Y. M. Sun, K. He, Z. F. Zhang, A. J. Zhou and H. W. Duan, *Biosens. Bioelectron.*, 2015, **68**, 358–364.
9 L. D. Deng, H. Miura, T. Shishido, Z. Wang, S. Hosokawa, K. Teramura and T. Tanaka, *J. Catal.*, 2018, **365**, 277–291.
10 S. Morales and A. Fernandez, *Int. J. Electrochem. Sci.*, 2013, **8**, 12692–12706.
11 Y. H. Qin, Z. Y. Xiong, J. Ma, Y. Li, Z. Wu, W. Feng, T. L. Wang, W. G. Wang and C. W. Wang, *Int. J. Hydrogen Energy*, 2016, **42**, 1103–1112.
12 L. Zhang, Y. He, X. Yang, H. Yuan, Z. Du and Y. Wu, *Chem. Eng. J.*, 2015, **278**, 129–133.

13 M. Hong, J. Li, W. Zhang, S. Liu and H. Chang, *Energy Fuels*, 2018, **32**, 6371–6377.
14 G. Xu, L. Yang, X. Wei, J. Ding, J. Zhong and P. K. Chu, *Adv. Funct. Mater.*, 2016, **26**, 3349–3358.
15 H. Yang, G. Xu, X. Wei, J. Cao, L. Yang and P. K. Chu, *J. Power Sources*, 2018, **395**, 295–304.
16 X. Zou, P. Xiong, J. Zhao, J. Hu, Z. Liu and Y. Xu, *Phys. Chem. Chem. Phys.*, 2017, **19**, 26495–26506.
17 N. Cai, J. Fu, H. Zeng, X. Luo, C. Han and F. Yu, *J. Alloys Compd.*, 2018, **742**, 769–779.
18 Y. Sun, Y. Cheng, K. He, A. Zhou and H. Duan, *RSC Adv.*, 2015, **5**, 10178–10186.
19 Y. Sun, Z. Fang, C. Wang, K. R. R. M. Ariyawansha, A. Zhou and H. Duan, *Nanoscale*, 2015, **7**, 7790–7801.
20 L. Peng, X. Peng, B. Liu, C. Wu, Y. Xie and G. Yu, *Nano Lett.*, 2013, **13**, 2151–2157.
21 L. Chu, W. Liu, A. Yu, Z. Qin, R. Hu, H. Shu, Q. P. Luo, Y. Min, J. Yang and X. A. Li, *Sol. Energy*, 2017, **153**, 584–589.
22 Y. Li, W. Xie, X. Hu, G. Shen, X. Zhou, Y. Xiang, X. Zhao and P. Fang, *Langmuir*, 2010, **26**, 591.
23 W. Li, Z. Wang, F. Deschler, S. Gao, R. H. Friend and A. K. Cheetham, *Nat. Rev. Mater.*, 2017, **2**, 16099.
24 P. Qin, G. Fang, W. Ke, F. Cheng, Q. Zheng, J. Wan, H. Lei and X. Zhao, *J. Mater. Chem. A*, 2014, **2**, 2742–2756.
25 W. Xiong, L. Zhou and S. Liu, *Chem. Eng. J.*, 2016, **284**, 650–656.
26 C. H. Zhu, F. P. Du, P. Fu, S. G. Wang and Z. D. Lin, *Mater. Res. Express*, 2018, **5**, 125016.
27 S. Zou, J. Luo, Z. Lin, P. Fu and Z. Chen, *Mater. Res. Express*, 2018, **5**, 125013.
28 C. Liu, J. Hong, Y. Zhang, Y. Zhao, L. Wang, L. Wei, S. Chen, G. Wang and J. Li, *Fuel*, 2016, **180**, 777–784.
29 X. Feng, H. Guo, K. Patel, H. Zhou and L. Xia, *Chem. Eng. J.*, 2014, **244**, 327–334.
30 Y. Gan, Y. Wei, J. Xiong and G. Cheng, *Chem. Eng. J.*, 2018, **349**, 1–16.
31 R. Wang, G. Cheng, Z. Dai, J. Ding, Y. Liu and R. Chen, *Chem. Eng. J.*, 2017, **327**, 371–386.
32 S. Luo, F. Qin, Y. Ming, H. Zhao, Y. Liu and R. Chen, *J. Hazard. Mater.*, 2017, **340**, 253.
33 J. Ke, X. Duan, S. Luo, H. Zhang, H. Sun, J. Liu, M. Tade and S. Wang, *Chem. Eng. J.*, 2017, **313**, 1447–1453.
34 X. Zou, Y. Dong, S. Li, J. Ke and Y. Cui, *Sol. Energy*, 2018, **169**, 392–400.
35 F. Chen, S. Xie, X. Huang and X. Qiu, *J. Hazard. Mater.*, 2017, **322**, 152–162.
36 Z. Du, F. Chen, Z. Lin, X. Li, H. Yuan and Y. Wu, *Chem. Eng. J.*, 2015, **278**, 79–84.
37 M. D. Merrill and R. C. Dougherty, *J. Phys. Chem. C*, 2008, **112**, 3655–3666.
38 R. D. Armstrong and M. F. Bell, *Electrochim. Acta*, 1978, **23**, 1111–1115.
39 R. Levy and M. Boudart, *Science*, 1973, **181**, 547–549.
40 X. Zou and Y. Zhang, *Chem. Soc. Rev.*, 2015, **44**, 5148–5180.
41 A. B. Laursen, S. Kegnæs, S. Dahl and I. Chorkendorff, *Energy Environ. Sci.*, 2012, **5**, 5577–5591.
42 E. J. Popczun, J. R. Mckone, C. G. Read, A. J. Biacchi, A. M. Wiltrout, N. S. Lewis and R. E. Schaak, *J. Am. Chem. Soc.*, 2013, **135**, 9267–9270.
43 J. Li, M. Hong, L. Sun, W. Zhang, H. Shu and H. Chang, *ACS Appl. Mater. Interfaces*, 2018, **10**, 458–467.
44 Y. Zhong, X. Xia, F. Shi, J. Zhan, J. Tu and H. Fan, *Adv. Sci.*, 2016, **3**, 1500286.
45 D. J. Ham and J. S. Lee, *Energies*, 2009, **2**, 873–899.
46 W. F. Chen, K. Sasaki, C. Ma, A. I. Frenkel, N. Marinkovic, J. T. Muckerman, Y. Zhu and R. R. Adzic, *Angew. Chem., Int. Ed.*, 2012, **51**, 6131–6135.
47 J. M. Jakšić, N. V. Krstajić, B. N. Grgur and M. M. Jakšić, *Int. J. Hydrogen Energy*, 1998, **23**, 667–681.
48 Y. Zhu, G. Chen, Y. Zhong, W. Zhou and Z. Shao, *Adv. Sci.*, 2018, **5**, 1700603.
49 S. Dong, X. Chen, X. Zhang and G. Cui, *Coord. Chem. Rev.*, 2013, **257**, 1946–1956.
50 J. S. J. Hargreaves, *Coord. Chem. Rev.*, 2013, **257**, 2015–2031.
51 B. Rauschenbach, A. Kolitsch and K. Hohmuth, *Phys. Status Solidi A*, 1983, **80**, 471–482.
52 N. Terada, Y. Hoshi, M. Naoe and S. Yamanaka, *IEEE Trans. Magn.*, 1984, **20**, 1451–1453.
53 R. Freer, *The Physics and Chemistry of Carbides, Nitrides and Borides*, Springer Science & Business Media, 2012.
54 E. Furimsky, *Appl. Catal., A*, 2003, **240**, 1–28.
55 J. W. Xiao, Y. Y. Xu, Y. T. Xia, J. B. Xi and S. Wang, *Nano Energy*, 2016, **24**, 121–129.
56 L. Li, X. Zhang, G. Wu, X. Peng, K. Huo and P. K. Chu, *Adv. Mater. Interfaces*, 2015, **2**, 1400446.
57 X. Peng, K. Huo, J. Fu, B. Gao, L. Wang, L. Hu, X. Zhang and P. K. Chu, *ChemElectroChem*, 2015, **2**, 512–517.
58 X. Peng, K. Huo, J. Fu, X. Zhang, B. Gao and P. K. Chu, *Chem. Commun.*, 2013, **49**, 10172–10174.
59 J. Wang, H. Liao, Y. Ji, F. Long, Y. Gu, Z. Zou, W. Wang and Z. Fu, *Beilstein J. Nanotechnol.*, 2017, **8**, 2116.
60 J. Xu, Z. Y. Li, Z. H. Xie and P. Munroe, *Scr. Mater.*, 2014, **74**, 88–91.
61 J. Song, G. Li, K. Xi, B. Lei, X. Gao and R. V. Kumar, *J. Mater. Chem. A*, 2014, **2**, 10041–10047.
62 L. Toth, *Transition metal carbides and nitrides*, Academic, New York, 1971.
63 V. A. Gubanov, A. L. Ivanovsky and V. P. Zhukov, *Electronic structure of refractory carbides and nitrides*, Cambridge University Press, 2005.
64 X. Peng, W. Li, L. Wang, L. Hu, W. Jin, A. Gao, X. Zhang, K. Huo and P. K. Chu, *Electrochim. Acta*, 2016, **214**, 201–207.
65 X. Peng, L. Wang, L. Hu, Y. Li, B. Gao, H. Song, C. Huang, X. Zhang, J. Fu, K. Huo and P. K. Chu, *Nano Energy*, 2017, **34**, 1–7.
66 X. Xiao, X. Peng, H. Jin, T. Li, C. Zhang, B. Gao, B. Hu, K. Huo and J. Zhou, *Adv. Mater.*, 2013, **25**, 5091–5097.
67 B. Gao, X. Li, X. Guo, X. Zhang, X. Peng, L. Wang, J. Fu, P. K. Chu and K. Huo, *Adv. Mater. Interfaces*, 2015, **2**, 1500211.
68 K. Schwarz, *Crit. Rev. Solid State Mater. Sci.*, 1987, **13**, 211–257.

69 P. Chen, K. Xu, Y. Tong, X. Li, S. Tao, Z. Fang, W. Chu, X. Wu and C. Wu, *Inorg. Chem. Front.*, 2016, **3**, 236–242.
70 V. Tagliazucca, K. Schlichte, F. Schüth and C. Weidenthaler, *J. Catal.*, 2013, **305**, 277–289.
71 E. Nurlaela, M. Harb, S. Del Gobbo, M. Vashishta and K. Takanabe, *J. Solid State Chem.*, 2015, **229**, 219–227.
72 H. Ju, D. Yu, L. Yu, N. Ding, J. Xu, X. Zhang, Y. Zheng, L. Yang and X. He, *Vacuum*, 2018, **148**, 54–61.
73 M. Senthil Kumar and J. Kumar, *Mater. Chem. Phys.*, 2003, **77**, 341–345.
74 G. Ma, Z. Wang, B. Gao, T. Ding, Q. Zhong, X. Peng, J. Su, B. Hu, L. Yuan and P. K. Chu, *J. Mater. Chem. A*, 2015, **3**, 14617–14624.
75 M. Harb, L. Cavallo and J.-M. Basset, *J. Phys. Chem. C*, 2014, **118**, 20784–20790.
76 A. Rizzo, M. Signore, L. Mirenghi, E. Piscopiello and L. Tapfer, *J. Phys. D: Appl. Phys.*, 2009, **42**, 235401.
77 J. Xu, L. L. Liu, P. Munroe and Z. H. Xie, *J. Mater. Chem. B*, 2015, **3**, 4082–4094.
78 J. Xu, S. Xu, P. Munroe and Z. H. Xie, *RSC Adv.*, 2015, **5**, 67348–67356.
79 O. Zsebök, J. Thordson, J. Gunnarsson, Q. Zhao, L. Ilver and T. Andersson, *J. Appl. Phys.*, 2001, **89**, 3662–3667.
80 E. Mohammadpour, Z. T. Jiang, M. Altarawneh, Z. H. Xie, Z. F. Zhou, N. Mondinos, J. Kimpton and B. Z. Dlugogorski, *Thin Solid Films*, 2016, **599**, 98–103.
81 W. T. Zheng, X. Wang, X. Kong, H. Tian, S. Yu, Z. Zhao and X. Li, *Powder Diffr.*, 2004, **19**, 352–355.
82 M. Benkahoul, E. Martinez, A. Karimi, R. Sanjinés and F. Lévy, *Surf. Coat. Technol.*, 2004, **180**, 178–183.
83 F. Yu, H. Zhou, Z. Zhu, J. Sun, R. He, J. Bao, S. Chen and Z. Ren, *ACS Catal.*, 2017, **7**, 2052–2057.
84 H. Yin, C. Zhang, F. Liu and Y. Hou, *Adv. Funct. Mater.*, 2014, **24**, 2930–2937.
85 W. Lengauer, *Transition Metal Carbides, Nitrides, and Carbonitrides*, Wiley-VCH Verlag GmbH, 2000.
86 J. S. Kang, M.-A. Park, J.-Y. Kim, S. H. Park, D. Y. Chung, S.-H. Yu, J. Kim, J. Park, J.-W. Choi and K. J. Lee, *Sci. Rep.*, 2015, **5**, 10450.
87 G. Dorman and M. Sikkens, *Thin Solid Films*, 1983, **105**, 251–258.
88 S. Xu, J. Xu, P. Munroe and Z. H. Xie, *Scr. Mater.*, 2017, **133**, 86–91.
89 J. J. Ma, J. Xu, S. Y. Jiang, P. Munroe and Z. H. Xie, *Ceram. Int.*, 2016, **42**, 16833–16851.
90 J. Cheng, J. Xu, L. L. Liu and S. Y. Jiang, *Materials*, 2016, **9**, 772.
91 J. Xu, W. Hu, Z. H. Xie and P. Munroe, *Surf. Coat. Technol.*, 2016, **296**, 171–184.
92 H. Deno, T. Kamemoto, S. Nemoto, A. Koshio and F. Kokai, *Appl. Surf. Sci.*, 2008, **254**, 2776–2782.
93 C. Giordano, C. Erpen, W. Yao and M. Antonietti, *Nano Lett.*, 2008, **8**, 4659–4663.
94 J. Wang, L. Grocholl and E. G. Gillan, *Nano Lett.*, 2002, **2**, 899–902.
95 X. Chen, J. Dye, H. Eick, S. Elder and K.-L. Tsai, *Chem. Mater.*, 1997, **9**, 1172–1176.
96 D. Xiang, Y. Liu, S. Gao and M. Tu, *Mater. Charact.*, 2008, **59**, 241–244.
97 D. Choi and P. N. Kumta, *J. Am. Ceram. Soc.*, 2007, **90**, 3113–3120.
98 L. Grocholl, J. Wang and E. G. Gillan, *Chem. Mater.*, 2001, **13**, 4290–4296.
99 Y. J. Han, X. Yue, Y. S. Jin, X. D. Huang and P. K. Shen, *J. Mater. Chem. A*, 2016, **4**, 3673–3677.
100 M. Shalom, D. Ressnig, X. Yang, G. Clavel, T. P. Fellinger and M. Antonietti, *J. Mater. Chem. A*, 2015, **3**, 8171–8177.
101 Y. Li, T. Takata, D. Cha, K. Takanabe, T. Minegishi, J. Kubota and K. Domen, *Adv. Mater.*, 2013, **25**, 125–131.
102 G. Liu, J. Shi, F. Zhang, Z. Chen, J. Han, C. Ding, S. Chen, Z. Wang, H. Han and C. Li, *Angew. Chem., Int. Ed.*, 2014, **53**, 7295–7299.
103 Y. Cong, H. S. Park, S. Wang, H. X. Dang, F. R. F. Fan, C. B. Mullins and A. J. Bard, *J. Phys. Chem. C*, 2012, **116**, 14541–14550.
104 M.-S. Balogun, Y. Huang, W. Qiu, H. Yang, H. Ji and Y. Tong, *Mater. Today*, 2017, **20**, 425–451.
105 D. Zhao, Z. Cui, S. Wang, J. Qin and M. Cao, *J. Mater. Chem. A*, 2016, **4**, 7914–7923.
106 H. Cui, G. Zhu, X. Liu, F. Liu, Y. Xie, C. Yang, T. Lin, H. Gu and F. Huang, *Adv. Sci.*, 2015, **2**, 1500126.
107 P. Qin, X. Li, B. Gao, J. Fu, L. Xia, X. Zhang, K. Huo, W. Shen and P. K. Chu, *Nanoscale*, 2018, **10**, 8728–8734.
108 C. Huang, Y. Yang, J. Fu, J. Wu, H. Song, X. Zhang, B. Gao, P. K. Chu and K. Huo, *J. Nanosci. Nanotechnol.*, 2018, **18**, 30–38.
109 W. Han, S. Fan, Q. Li and Y. Hu, *Science*, 1997, **277**, 1287–1289.
110 X. Lu, M. Yu, T. Zhai, G. Wang, S. Xie, T. Liu, C. Liang, Y. Tong and Y. Li, *Nano Lett.*, 2013, **13**, 2628–2633.
111 D. Choi, G. E. Blomgren and P. N. Kumta, *Adv. Mater.*, 2006, **18**, 1178–1182.
112 L. Volpe and M. Boudart, *J. Solid State Chem.*, 1985, **59**, 332–347.
113 S.-H. Kim, J.-K. Kim, N. Kwak, H. Sohn, J. Kim, S.-H. Jung, M.-R. Hong, S. H. Lee and J. Collins, *Electrochem. Solid-State Lett.*, 2006, **9**, C54–C57.
114 X. Jia, Y. Zhao, G. Chen, L. Shang, R. Shi, X. Kang, G. I. Waterhouse, L. Z. Wu, C. H. Tung and T. Zhang, *Adv. Energy Mater.*, 2016, **6**, 1502585.
115 J. Jia, M. Zhai, J. Lv, B. Zhao, H. Du and J. Zhu, *ACS Appl. Mater. Interfaces*, 2018, **10**, 30400–30408.
116 Y. Li, L. Hu, W. Zheng, X. Peng, M. Liu, P. K. Chu and L. Y. S. Lee, *Nano Energy*, 2018, **52**, 360–368.
117 X. Xiao, H. Yu, H. Jin, M. Wu, Y. Fang, J. Sun, Z. Hu, T. Li, J. Wu and L. Huang, *ACS Nano*, 2017, **11**, 2180–2186.
118 X. Xiao, H. Song, S. Lin, Y. Zhou, X. Zhan, Z. Hu, Q. Zhang, J. Sun, B. Yang and T. Li, *Nat. Commun.*, 2016, **7**, 11296.
119 N. Li, G. Yang, Y. Sun, H. Song, H. Cui, G. Yang and C. Wang, *Nano Lett.*, 2015, **15**, 3195–3203.
120 B. Liu, X. Zhou and H. D. Li, *Phys. Status Solidi A*, 1989, **113**, 11–22.
121 J. R. Conrad, J. Radtke, R. Dodd, F. J. Worzala and N. C. Tran, *J. Appl. Phys.*, 1987, **62**, 4591–4596.

122 H. Y. Zhao, Z. R. Fan, Q. M. Fu, H. Wang, Z. Hu, H. Tao, X. D. Zhang, Z. B. Ma and T. T. Jia, *J. Mater. Sci.*, 2018, **53**, 15340–15347.

123 Y. Zhang, B. Ouyang, J. Xu, G. Jia, S. Chen, R. S. Rawat and H. J. Fan, *Angew. Chem., Int. Ed.*, 2016, **55**, 8670–8674.

124 Y. Zhang, B. Ouyang, J. Xu, S. Chen, R. S. Rawat and H. J. Fan, *Adv. Energy Mater.*, 2016, **6**, 1600221.

125 D. Mao, K. Tao and J. Hopwood, *J. Vac. Sci. Technol., A*, 2002, **20**, 379–387.

126 R. Rawat, W. Chew, P. Lee, T. White and S. Lee, *Surf. Coat. Technol.*, 2003, **173**, 276–284.

127 D. Nolan, S. W. Huang, V. Leskovsek and S. Braun, *Surf. Coat. Technol.*, 2006, **200**, 5698–5705.

128 I. Neklyudov and A. Morozov, *Phys. B*, 2004, **350**, 325–337.

129 J.-S. Park, M.-J. Lee, C.-S. Lee and S.-W. Kang, *Electrochem. Solid-State Lett.*, 2001, **4**, C17–C19.

130 J. Xu, J. J. Ma, P. Munroe and Z.-H. Xie, *Surf. Rev. Lett.*, 2018, **25**, 1850083.

131 S. Xu, P. Munroe, J. Xu and Z.-H. Xie, *Surf. Coat. Technol.*, 2016, **307**, 470–475.

132 R. Molnar and T. Moustakas, *J. Appl. Phys.*, 1994, **76**, 4587–4595.

133 S. Tanaka, R. S. Kern and R. F. Davis, *Appl. Phys. Lett.*, 1995, **66**, 37–39.

134 L. Rosenberger, R. Baird, E. McCullen, G. Auner and G. Shreve, *Surf. Interface Anal.*, 2008, **40**, 1254–1261.

135 X. X. Zou and Y. Zhang, *Chem. Soc. Rev.*, 2015, **44**, 5148–5180.

136 Y. Lee, J. Suntivich, K. J. May, E. E. Perry and Y. Shao-Horn, *J. Phys. Chem. Lett.*, 2015, **3**, 399–404.

137 T. Reier, M. Oezaslan and P. Strasser, *ACS Catal.*, 2012, **2**, 1765–1772.

138 M. Tahir, N. Mahmood, L. Pan, Z.-F. Huang, Z. Lv, J. Zhang, F. K. Butt, G. Shen, X. Zhang and S. X. Dou, *J. Mater. Chem. A*, 2016, **4**, 12940–12946.

139 Y. Li, P. Hasin and Y. Wu, *Adv. Mater.*, 2010, **22**, 1926–1929.

140 Y. Meng, W. Song, H. Huang, Z. Ren, S.-Y. Chen and S. L. Suib, *J. Am. Chem. Soc.*, 2014, **136**, 11452–11464.

141 J. X. Feng, S. H. Ye, H. Xu, Y. X. Tong and G. R. Li, *Adv. Mater.*, 2016, **28**, 4698–4703.

142 R. Chen, H.-Y. Wang, J. Miao, H. Yang and B. Liu, *Nano Energy*, 2015, **11**, 333–340.

143 M. Shalom, V. Molinari, D. Esposito, G. Clavel, D. Ressnig, C. Giordano and M. Antonietti, *Adv. Mater.*, 2014, **26**, 1272–1276.

144 B. Cao, G. M. Veith, J. C. Neuefeind, R. R. Adzic and P. G. Khalifah, *J. Am. Chem. Soc.*, 2013, **135**, 19186–19192.

145 X. Peng, A. M. Qasim, W. Jin, L. Wang, L. Hu, Y. Miao, W. Li, Y. Li, Z. Liu, K. Huo, K.-y. Wong and P. K. Chu, *Nano Energy*, 2018, **53**, 66–73.

146 J. Xie, S. Li, X. Zhang, J. Zhang, R. Wang, H. Zhang, B. Pan and Y. Xie, *Chem. Sci.*, 2014, **5**, 4615–4620.

147 A. P. Murthy, D. Govindarajan, J. Theerthagiri, J. Madhavan and K. Parasuraman, *Electrochim. Acta*, 2018, **283**, 1525–1533.

148 W.-F. Chen, J. T. Muckerman and E. Fujita, *Chem. Commun.*, 2013, **49**, 8896–8909.

149 V. Chakrapani, J. Thangala and M. K. Sunkara, *Int. J. Hydrogen Energy*, 2009, **34**, 9050–9059.

150 J. Shi, Z. Pu, Q. Liu, A. M. Asiri, J. Hu and X. Sun, *Electrochim. Acta*, 2015, **154**, 345–351.

151 B. Ren, D. Li, Q. Jin, H. Cui and C. Wang, *J. Mater. Chem. A*, 2017, **5**, 19072–19078.

152 K. Xu, P. Z. Chen, X. L. Li, Y. Tong, H. Ding, X. J. Wu, W. S. Chu, Z. M. Peng, C. Z. Wu and Y. Xie, *J. Am. Chem. Soc.*, 2015, **137**, 4119–4125.

153 L. Ma, L. R. L. Ting, V. Molinari, C. Giordano and B. S. Yeo, *J. Mater. Chem. A*, 2015, **3**, 8361–8368.

154 W.-F. Chen, S. Iyer, S. Iyer, K. Sasaki, C.-H. Wang, Y. Zhu, J. T. Muckerman and E. Fujita, *Energy Environ. Sci.*, 2013, **6**, 1818–1826.

155 S. W. Li, Y. C. Wang, S. J. Peng, L. J. Zhang, A. M. Al-Enizi, H. Zhang, X. H. Sun and G. F. Zheng, *Adv. Energy Mater.*, 2016, **6**, 1501661.

156 H. J. Yan, C. G. Tian, L. Wang, A. P. Wu, M. C. Meng, L. Zhao and H. G. Fu, *Angew. Chem., Int. Ed.*, 2015, **54**, 6325–6329.

157 Y. Y. Wang, C. Xie, D. D. Liu, X. B. Huang, J. Huo and S. Y. Wang, *ACS Appl. Mater. Interfaces*, 2016, **8**, 18652–18657.

158 Y. Wang, D. Liu, Z. Liu, C. Xie, J. Huo and S. Wang, *Chem. Commun.*, 2016, **52**, 12614–12617.

159 B. Zhang, C. Xiao, S. Xie, J. Liang, X. Chen and Y. Tang, *Chem. Mater.*, 2016, **28**, 6934–6941.

160 P. Z. Chen, K. Xu, Z. W. Fang, Y. Tong, J. C. Wu, X. L. Lu, X. Peng, H. Ding, C. Z. Wu and Y. Xie, *Angew. Chem., Int. Ed.*, 2015, **54**, 14710–14714.

161 F. Y. Xie, H. L. Wu, J. R. Mou, D. M. Lin, C. G. Xu, C. Wu and X. P. Sun, *J. Catal.*, 2017, **356**, 165–172.

162 J. K. Nørskov, T. Bligaard, A. Logadottir, J. Kitchin, J. G. Chen, S. Pandelov and U. Stimming, *J. Electrochem. Soc.*, 2005, **152**, J23–J26.

163 A. Ignaszak, C. Song, W. Zhu, J. Zhang, A. Bauer, R. Baker, V. Neburchilov, S. Ye and S. Campbell, *Electrochim. Acta*, 2012, **69**, 397–405.

164 Y. Liu, T. G. Kelly, J. G. Chen and W. E. Mustain, *ACS Catal.*, 2013, **3**, 1184–1194.

165 J. Deng, H. Li, J. Xiao, Y. Tu, D. Deng, H. Yang, H. Tian, J. Li, P. Ren and X. Bao, *Energy Environ. Sci.*, 2015, **8**, 1594–1601.

166 E. Navarro-Flores, Z. Chong and S. Omanovic, *J. Mol. Catal. A: Chem.*, 2005, **226**, 179–197.

167 B. Wei, G. Tang, H. Liang, Z. Qi, D. Zhang, W. Hu, H. Shen and Z. Wang, *Electrochem. Commun.*, 2018, **93**, 166–170.

168 Y. Wang, B. Zhang, W. Pan, H. Ma and J. Zhang, *ChemSusChem*, 2017, **10**, 4170–4177.

169 F. Yan, Y. Wang, K. Li, C. Zhu, P. Gao, C. Li, X. Zhang and Y. Chen, *Chem.–Eur. J.*, 2017, **23**, 10187–10194.

170 Y. Liang, Y. Li, H. Wang, J. Zhou, J. Wang, T. Regier and H. Dai, *Nat. Mater.*, 2011, **10**, 780–786.

171 X. Peng, L. Hu, L. Wang, X. Zhang, J. Fu, K. Huo, S. L. Y. Lee, K.-Y. Wong and P. K. Chu, *Nano Energy*, 2016, **26**, 603–609.

172 Z. Guo, X. Feng, X. Li, X. Zhang, X. Peng, H. Song, J. Fu, K. Ding, X. Huang and B. Gao, *Front. Chem.*, 2018, **6**, 429.

173 Y. Zhu, G. Chen, X. Xu, G. Yang, M. Liu and Z. Shao, *ACS Catal.*, 2017, **7**, 3540–3547.

174 Z. Lv, M. Tahir, X. Lang, G. Yuan, L. Pan, X. Zhang and J.-J. Zou, *J. Mater. Chem. A*, 2017, **5**, 20932–20937.
175 K. Ojha, S. Banerjee and A. K. Ganguli, *J. Chem. Sci.*, 2017, **129**, 989–997.
176 Z. Chen, Y. Ha, Y. Liu, H. Wang, H. Yang, H. Xu, Y. Li and R. Wu, *ACS Appl. Mater. Interfaces*, 2018, **10**, 7134–7144.
177 A. Morozan, V. Goellner, A. Zitolo, E. Fonda, B. Donnadieu, D. Jones and F. Jaouen, *Phys. Chem. Chem. Phys.*, 2015, **17**, 4047–4053.
178 W. F. Chen, J. M. Schneider, K. Sasaki, C. H. Wang, J. Schneider, S. Iyer, S. Iyer, Y. Zhu, J. T. Muckerman and E. Fujita, *ChemSusChem*, 2014, **7**, 2414–2418.
179 R. Kumar, R. Rai, S. Gautam, A. De Sarkar, N. Tiwari, S. N. Jha, D. Bhattacharyya, A. K. Ganguli and V. Bagchi, *J. Mater. Chem. A*, 2017, **5**, 7764–7768.
180 J. Wang, W. Chen, T. Wang, N. Bate, C. Wang and E. Wang, *Nano Res.*, 2018, **11**, 4535–4548.
181 S. Wang, H. Ge, S. Sun, J. Zhang, F. Liu, X. Wen, X. Yu, L. Wang, Y. Zhang and H. Xu, *J. Am. Chem. Soc.*, 2015, **137**, 4815–4822.